Palaeogeography Palaeoclimatology Palaeoecology
May 2018, Volume 496 Pages 225-237
https://doi.org/10.1016/j.palaeo.2018.01.040
https://archimer.ifremer.fr/doc/00616/72791/

Variations in benthic foraminiferal assemblages in the Tagus mud belt during the last 5700 years: Implications for Tagus River discharge

Dessandier Pierre-Antoine [1, *], Bonnin Jerome [1], Malaize Bruno [1], Lambert Clement [2], Tjallingii Rik [3, 5], Warden Lisa [3], Damste Jaap S. Sinninghe [3, 4], Kim Jung-Hyun [3, 6]

[1] Univ Bordeaux, CNRS, UMR EPOC 5805, Allee Geoffroy St Hilaire, F-33615 Pessac, France.
[2] Univ Bretagne Occidentale, Lemar UMR 6539, IUEM Technopole Brest Iroise,Rue Dumont dUrville, F-29280 Plouzane, France.
[3] Univ Utrecht, NIOZ Royal Netherlands Inst Sea Res, Dept Marine Microbiol & Biogeochem, NL-1790 AB Utrecht, Netherlands.
[4] Univ Utrecht, Dept Geosci, Fac Earth Sci, POB 80-021, Utrecht, Netherlands.
[5] GFZ German Res Ctr Geosci, Climate Dynam & Landscape Evolut, Potsdam, Germany.
[6] Korea Polar Res Inst, 26 Songdomirae Ro, Incheon 21990, South Korea.

* Corresponding author : Pierre-Antoine Dessandier, email address : pierre-antoine.dessandier@uit.no

Abstract :

We analyzed a 10-m sediment core retrieved at 82 m water depth off the coast of the Tagus River (Western Iberian Margin, Portugal) to investigate a linkage between variations in benthic foraminiferal assemblages and Tagus River discharge over the last 5700 years. Benthic foraminiferal assemblages were studied at high resolution in combination with the stable carbon and oxygen isotopic composition of fossil shells of Nonion scaphum, bulk and molecular organic matter properties (TOC, TN, C/N ratio, delta C-13(TOC), delta N-15(bulk), and BIT index), magnetic susceptibility, and XRF analyses. Three periods of environmental changes were identified: 1) high Tagus River discharge in 5750-2200 calendar year before present (cal yr BP), 2) lower discharge characterized by intense upwelling conditions (2250-1250 cal yr BP), and 3) both intense upwelling and Tagus River discharge (1250 cal yr BP-present). The data reveal alternating intense upwelling periods, as shown by the dominance of Cassidulina carinata, Valvulineria bradyana, or Bulimina marginata, whereas periods of increased river discharge are indicated by increase of N. scaphum, Ammonia beccarii, and Planorbulina mediterranensis. The Tagus River discharge was the strongest during the first period, transporting riverine material further offshore and preventing the establishment of a mud belt on the mid-shelf (around 100 m depth). During the second period, a decrease in Tagus River discharge favored the formation of the Tagus mud belt and strongly influenced the benthic environment by creating an organic matter stock. During the third period, intense upwelling and increased Tagus River discharge were recorded by benthic foraminiferal distribution, with an increase of terrestrial elements present in the mud belt. Furthermore, our results showed that variations in benthic foraminiferal assemblages corresponded to the well-known climatic periods in the study area, such as the Roman Period, the Dark Ages, the Medieval Warm Period, and the Little Ice Age. Our study

strongly suggests that benthic foraminiferal assemblages can be used as a bio-indicator to trace the influence of past river discharge.

Highlights

► Benthic foraminifera allow the reconstruction of past Tagus River discharges. ► Three different periods of environmental changes have been identified. ► Major change is due to the Tagus mud belt onset at around 2000 yr BP. ► Upwelling active periods are linked with positive phases of NAO. ► Tagus River discharges are associated with negative phases of NAO.

Keywords : Holocene, Portuguese Margin, Paleo-reconstruction, North Atlantic Oscillation

1. Introduction

In the last decades, benthic foraminiferal assemblages have often been used in paleoceanography to investigate biostratigraphy, paleobathymetry, and abiotic conditions, such as temperature, salinity, and pH (Jorissen et al., 2007 and references therein). The TROX model (Jorissen et al., 1995) established that oxygen concentration and organic matter content in the sediment are the major environmental controls on the distribution of benthic foraminifera in marine sediments. Subsequent studies emphasized the importance of the quality of the organic matter for the composition of living benthic foraminifera faunas in various marine environments (e.g., Goldstein and Corliss, 1994; Suhr et al., 2003; Fontanier et al., 2005, Goineau et al., 2011, Dessandier et al., 2015). Benthic foraminifera are known to bloom following high marine algal production (e.g., Kitazato et al., 2000). After a phytoplankton bloom, benthic foraminifera respond rapidly to the increased influx of fresh organic matter (Fontanier et al., 2003). Terrestrial input may also impact the organic matter supply and its quality and thereby may partly control the benthic foraminiferal distribution in continental shelf sediments. This is particularly true for river-dominated shelves where living benthic foraminifera have been identified to respond to river inputs (e.g., Mendes et al., 2004; Mojtahid et al., 2009; Goineau et al., 2011).

Dessandier et al. (2016, 2018) have shown through studies on living and dead faunas that some species could be used as bio-indicators of river discharge and upwelling intensity in the Portuguese Margin. During the last millennia, these environmental conditions were influenced by rapid climatic changes (Abrantes et al., 2005, Lebreiro et al., 2006). Within the Quaternary, the Holocene is characterized by relatively stable climatic conditions with millennial-scale variability (Bond et al., 1997). The solar variability superimposed on long-term

changes in insolation seems to be one of the most likely important forcing mechanisms for the rapid climate changes over the Holocene (Mayewski et al., 2004). The North Atlantic Oscillation (NAO) was also described as a major factor for the variability of climate in Europe (Wanner et al., 2001), which played an important role in the control of the upwelling intensity and humidity of the Iberian Peninsula (Abrantes et al., 2005; Lebreiro et al., 2006; Fig. 1). The NAO is an atmospheric process characterized by a seesaw between the Icelandic low and the Azores high pressures. The positive mode (NAO+) is characterized by well-developed Icelandic low and Azores high pressures, associated with stronger westerlies over the eastern North Atlantic and the European continent. The negative mode (NAO-) is characterized by a rather weak pressure seesaw and reduced westerlies (Wanner et al., 2001). The last millennia were marked by short-scale climatic changes, mainly controlled by solar activity and NAO-like processes. Several such periods of short-scale changes were identified, among them the Roman Period (RP; e.g., Lamb, 1985), the Dark Ages (DA; e.g., Keigwin and Pickart, 1999), the Medieval Warm Period (MWP), the Little Ice Age (LIA; deMenocal et al., 2000; Trouet et al., 2009), and a warming during the twentieth century determined by instrumental temperature measurements of the last two centuries. The major climatic changes, MWP and LIA, have been described as controlled by NAO+ and NAO-, respectively (Lebreiro et al., 2006; Trouet et al., 2009). The nature and chronology of these events are still debated (Desprat et al., 2003; Ortega et al., 2015; Swingedouw et al., 2015), but the influence of these abrupt changes on the rainfall and upwelling intensity has been observed in the Iberian Margin (Abrantes et al., 2005; Bartels-Jónsdóttir et al., 2006). During the NAO- mode, the Iberian Margin is marked by increased humidity, which is responsible for strengthened riverine discharge (Bernárdez et al., 2008). The NAO+ mode is characterized by an increase in Iberian coastal upwelling (Lebreiro et al., 2006). Another oscillation, called the Atlantic Multidecadal Oscilllation (Kerr, 2000), was also

described as a controlling factor of rainfall during the last century that had a greater influence on the American continent, Sahel, and northern Europe (Knight al., 2006).

We tested the applicability of these benthic foraminifera as bio-indicators of past upwelling intensity and changes in river discharge on a late Holocene sediment sequence from the Tagus prodelta. We used a multiproxy approach based on organic parameters (total organic carbon [TOC], total nitrogen [TN], C/N ratio, $\delta^{15}N_{bulk}$, and $\delta^{13}C_{TOC}$), XRF data, benthic foraminiferal assemblages, and carbon and oxygen stable isotopes of benthic foraminifera to compare climatic changes of the late Holocene with river regime change. The branched isoprenoid tetraethers (BIT) index was measured in the core that was previously published in Warden et al. (2016) and compared with our reconstruction. We applied our reconstruction on a paleoclimatological record never studied at this water depth, under the influence of the Tagus River, and provided a new dataset to improve understanding of the effect of NAO-like processes during the Holocene.

2. Study area

Our study area was located at the mid-shelf off the Tagus River mouth, on the western Iberian Margin (Fig. 1) which is a narrow (20–34 km) shelf (Dias et al., 2002) that extends from 37ºN to 42ºN latitude. The shelf break is located at 140 m depth, on the outer continental shelf and slope, and three main submarine troughs (the Cascais Canyon, Lisbon Canyon, and Setùbal Canyon) are related to geological features (Jouanneau et al., 1998). The regional hydrodynamic regime is driven by the influence of wave action, tidal and rip currents, and storm surges, which plays a role in determining the particle size distribution on shelf sediments (Oliveira et al., 2007). However, the Tagus area is protected against swell from the northwest (Jouanneau et al., 1998). Sandy deposits occur on the inner shelf, where there are high-energy littoral currents. The dominant regional surface current (the Portugal Coastal Counter Current) flows southward

and transports material from the shelf to the deep ocean during winter storms (Vitorino et al., 2002b). The outer shelf is affected by internal waves, especially during periods when water masses are stratified, resulting in the deposition of large bodies of sandy and gravelly sands (Jouanneau et al., 1998). The export of terrestrial sediment and nutrients along the shelf is predominantly influenced by sediment supplied by three main rivers: the Douro, Tagus, and Sado (Jouanneau et al., 1998; Dias et al., 2002). At around 100 m water depth, the finest particles are deposited in accumulation areas, called the mud belt (or mud patch). The mud belt lies beyond the line where seasonal thermal stratification of surface waters occurs, especially off the mouths of the Douro and Tagus rivers (Jouanneau et al., 1998; Dias et al., 2002). These accumulation zones are composed of mixed sources of marine, estuarine, and terrestrial organic matter (Schmidt et al., 2010). Winter storms can remobilize the sediment and transport it northward by the action of bottom currents (Dias et al., 2002; Vitorino et al., 2002a), eventually depositing it on the mid-shelf mud belt between 50 and 130 m water depth (Vitorino et al., 2002b).

The Eastern North Atlantic Central Water (ENACW) is a slope current characterized by a decrease of salinity under the surface currents, with a minimum of 35.6 at 450–500 m water depth (Oliveira et al., 2007). The ENACW is upwelled during summer. Between May and September, the Azores high-pressure system is driven closer to the coast. Together with the associated northerly winds, this atmospheric system makes the colder, less salty, and nutrient-enriched subsurface water (60–120 m water depth) rise to the surface along the Iberian Margin (Fiúza, 1983). This upwelling leads to an increased productivity in the summer along a 50-km-wide zone. The main upwelling front is oriented along the bathymetry off the 100 m isobath in the northern part of the Iberian Peninsula; it then turns slightly offshore and southward (Peliz et al., 2002). Most of the primary producers, especially cyanobacteria and diatoms, that are dominant in the Iberian Margin increase during upwelling events (Tilstone et al., 2003). Active

upwelling periods have a large impact on marine trophic conditions in this area (Fiúza, 1983) and are characterized by maximal organic carbon exports to the seafloor (Jouanneau et al., 1998). Periods of strong Iberian river discharge that occur during phases when upwelling is reduced are characterized by a substantially increased export of continental nutrients, which triggers phytoplankton production (Prieto et al., 2009; Rodrigues et al., 2009). To a lesser extent, phytoplanktonic blooms occur in November and between April and May (Ferreira and Duarte, 1994). In winter, the Azores high-pressure system moves south, which results in southerly winds and downwelling conditions that lead to the deposition of sediments on the shelf (Frouin et al., 1990). Upwelling activity and fluvial discharge are consequently the two major parameters controlling the marine biology on the Iberian Shelf (Lebreiro et al., 2006) due to their impact on the deposition of organic matter, which is important for benthic organisms.

The Tagus is the longest (1,008 km) Iberian river in the central part of the Peninsula and has a large mesotidal estuary with an area of 340 km^2 (Vale and Sundby, 1987). The Tagus watershed is about 80,600 km^2 and has an annual mean water discharge of 360 $m^3 s^{-1}$ (Jouanneau et al.,1998), with strong seasonal changes in discharge from 1 to 2,200 $m^3 s^{-1}$ (Atlas Nacional de España), controlled by maximal rainfall in winter (Aguiar and Ferreira, 2005; Azevedo et al., 2008). The Tagus River flows were largely modulated by the NAO during the last century (Trigo et al., 2004) and the last millennia (e.g., Abrantes et al., 2005; Bartels-Jónsdóttir et al., 2006; Lebreiro et al., 2006). The river discharge also controls the input of chlorophyll associated with phytodetritic material in the marine environment and the water column stratification (Relvas et al., 2007).

3. Material and methods

Core 64PE332-30-2 was obtained in March 2011 during the Pacemaker 64PE332 cruise on board the R/V *Pelagia* (38°39’04’’N, 9°28’13’’W). This 978-cm Kullenberg piston core

was retrieved from the Tagus mud belt at 82 m water depth (Fig. 1). Sediment slices 1 or 2 cm thick were sampled every 10 cm, dried, weighted, and washed through 63 and 150 µm sieves. For this study, 101 samples of >150 µm benthic foraminifera were handpicked and placed in Chapman cells before taxonomic identification under a stereomicroscope. After splitting using an Otto microsplitter, a minimum of 250 specimens were counted. Diversity indices (Shannon [S] and Evenness indices) were calculated using the PAleontological STatistics (PAST) software (Version 2.14; Hammer et al., 2001). The benthic foraminiferal number (BFN), which represents the number of individuals per analyzed dry sediment mass, was calculated for all samples.

Isotopic analyses were performed on monospecific samples of the benthic foraminiferal species *Nonion scaphum*, which is present all along the core and is typical of the Iberian mud belt (Dessandier et al., 2015; 2016), at the EPOC laboratory, University of Bordeaux. This species was observed alive below the oxygen penetration, between 1 and 2 cm depth in the mud belt area (Dessandier et al., 2016), suggesting that it may reflect subsurface sediment pore water rather than bottom water conditions. However, we compared only the data measured on the same species in every sample, avoiding any bias from the early diagenesis effect for environmental reconstruction. For each sample, three or four specimens were handpicked and dissolved in acid via the Micromass Multiprep autosampler system. The resulting carbon dioxide gas was analyzed against the international reference standard NBS 19 ($\delta^{13}C$ = + 1.96 ‰ / PDB and $\delta^{18}O$ = – 2.20 ‰ / PDB) using an Optima Micromass mass spectrometer. Measurements were taken for each depth horizon (1 cm) in triplicate to reduce uncertainties. The analytical precision was better than 0.05 ‰ for $\delta^{18}O$ and 0.03 ‰ for $\delta^{13}C$.

The age model for the sediment core, modified according to Warden et al. (2016), was based on the magnetic susceptibility (MS) and seven accelerated mass spectrometry (AMS) ^{14}C radiocarbon dates (Table 1). The MS record of Core 64PE332-30-2 was compared with that of

175 Core GeoB 8903 (Abrantes et al., 2008), which was also retrieved in the Tagus prodelta at ~100
176 m water depth (Fig. 1). Table 1 summarizes the ^{14}C AMS dating points of the two cores
177 considered in this study. Because of the low number of dating points in the upper part of Core
178 64PE332-30-2, we compared our record of MS and age model with Core GeoB 8903, which
179 had a substantial number of ^{14}C AMS dating points in the upper section (Figs. 2 and 3). The
180 MS was measured on board at 5-cm intervals using a Bartington MS meter with a 12-cm
181 diameter loop. The final age model was achieved by a linear interpolation between each AMS
182 ^{14}C age. The ^{14}C data calibration was made via the program CALIB V0.6 with the Marine13
183 calibration curve (Stuiver and Reimer, 1993), using the common reservoir age of 400 years
184 because no regional effect on reservoir age is known in our sampling area (Abrantes et al.,
185 2005). AMS ^{14}C ages and the dating points of GeoB8903 were converted to cal yr BP.

186 Core 64PE332-30-2 was scanned with an Avaatech XRF core scanner at NIOZ at 1-cm
187 resolution. Detailed bulk-chemical composition records acquired by XRF core scanning allow
188 accurate determination of stratigraphical changes and assessment of the contribution of the
189 various components in lithogenic and marine sediments (Stuut et al., 2014). The XRF core
190 scanner uses energy dispersive fluorescence radiation to measure the chemical composition of
191 the sediment as element intensities in total counts or counts per second (Tjallingii et al., 2007).
192 After cleaning and preparation of the archive-halve core surface and covering with SPEX Certi
193 Ultralene® foil, the core was measured at both 10 kV and 30 kV. Element intensities are
194 presented as log ratios that are normally distributed and linearly related to log ratios of element
195 concentration (Weltje and Tjallingii, 2008). Terrestrial exports, such as metals or contaminants,
196 are indicated mainly by Fe/Ti and Pb/Ti ratios. The Zr/Rb ratio serves as a grain size indicator
197 (Taylor, 1965), and the Br/Cl ratio indicates organic sediment (Ziegler et al., 2008).

198 Sediments were freeze-dried and ground before the geochemical analyses. TN and $\delta^{15}N$
199 were measured with a Thermo-Scientific Flash 2000 Elemental Analyzer interfaced at NIOZ.

The analyses were determined at least in duplicate and the analytical error was, on average, smaller than 0.1 wt. % for the TN content. The TOC content, the stable carbon isotopic composition of TOC ($\delta^{13}C_{TOC}$), and BIT data were previously published by Warden et al. (2016). The C/N ratio was calculated as the division of TOC/TN.

A principal component analysis (PCA) was performed on 22 samples of normalized environmental and faunal data, using PRIMER version 6.0 software (Clarke and Warwick, 1994) to compare the response of the faunal and environmental parameters. The two major PCA scores were plotted to define the different phases of the reconstruction.

4. Results

4.1. Sedimentological features and age model

The final age model of Core 64PE332-30-2 (Fig. 3) revealed that the sedimentation rates were increasing over time, with a first phase of ~0.06 cm/yr^{-1} from 5750 to 2200 cal yr BP. In a second phase, 2200-present, the sedimentation rate was ~ 0.52 cm yr^{1}. The MS record and grain size distribution of the Core GeoB 8903 were plotted as a function of age, and the MS and Ca/Ti record of Core 64PE332-30-2 were plotted as a function of core depth (Fig. 2). Similar trend signals in the MS records were identified in the two cores, and the Ca/Ti record measured by XRF showed a similar trend to the grain size record of core GeoB 8903. The MS record showed three phases, with the first characterized by an increase of MS at 770 cm sediment core depth, the second a larger increase at around 400 cm, and the third a more stable trend until the end. This trend was opposite that of the Ca/Ti content, which revealed two successive decreases of values at the same depths.

4.2. Environmental change phases

XRF, organic matter, and benthic foraminiferal isotopes data are plotted in Fig. 4. Three phases appeared following the environmental changes, mainly determined by the XRF ratios. Phase I (575-2250 cal yr BP) was characterized by high Zr/Rb and Ca/Ti counts, while the Br/Cl and Fe/Ti counts were low. The BIT index was low and stable (below ~ 0.04), the TOC content was also stable at around 0.9 wt. %, $\delta^{13}C_{TOC}$ was about – 24.3 ‰, and $\delta^{15}N_{bulk}$ was about + 3.9 ‰ (Warden et al., 2016). The TN was the only organic parameter that slightly increased during this phase, from 0.04 to 0.08 wt. % (Warden et al., 2016). The C/N ratio showed an opposite trend, with a clear decrease from 18 to 11. Both the carbon and oxygen stable isotope composition of *N. scaphum* slightly decreased during this interval, $\delta^{18}O_{bf}$ from + 1.7 to + 1.4 ‰ and $\delta^{13}C_{bf}$ from – 1.1 to – 1.2 ‰.

Phase II (2250-1250 cal yr BP) was characterized by a rapid decrease in Ca/Ti and Zr/Rb counts, a strong increase in Br/Cl counts, and a slight increase in Fe/Ti. The BIT index increased slightly, to 0.06. The TOC, $\delta^{13}C_{TOC}$, and C/N ratio reached high values at the end of the period (around 1.5 wt. %, – 23.0 ‰, and 16, respectively) after a large increase. TN and $\delta^{15}N_{bulk}$ showed a smaller increase; TN moved from 0.9 to 0.13 wt. % and $\delta^{15}N_{bulk}$ from + 3.6 to + 3.9 ‰. Isotopes measured on benthic foraminifera became more variable at the beginning of the period, and this trend continued until the end of the record. The decrease in $\delta^{13}{}_{bf}$ observed in phase I was stronger, and $\delta^{18}O_{bf}$ remained fairly constant.

Phase III (1250 cal yr BP-present) was characterized by a continued decrease of Ca/Ti counts and a large decrease of Zr/Rb counts. Br/Cl counts were also unstable and lacking any clear trend. The Fe/Ti and Pb/Ti counts from Phase III showed an increase until the end of the record, especially during the last 500 years for Pb/Ti, after a stable trend during the two previous phases. They both peaked at 250 cal yr BP, when Br/Cl decreased. The TOC content, $\delta^{13}C_{TOC}$, and C/N ratio decreased, to 1.2 wt. %, – 24 ‰, and 8, respectively. The $\delta^{13}C_{TOC}$ and TOC increased during the last 200 years, reaching – 28.8 ‰ and 1.2 wt. %, respectively. TN and

249 $\delta^{15}N_{bulk}$ were roughly constant before a large increase at the end of the period, reaching 0.17 %
250 and + 4.7 ‰, respectively. The $\delta^{18}O_{bf}$ increased at the beginning from + 1.3 to + 1.8 ‰ and
251 decreased until + 1.5 ‰ at the end; $\delta^{13}C_{bf}$ showed the opposite trend, with a large decrease from
252 – 1.5 to – 3.5 ‰. The C/N ratio was slightly decreasing from the start of this period until the
253 present. Conversely, the BIT index was progressively increasing, reaching 0.12, but dropped in
254 the most recent sediment horizon analyzed.
255
256 4.3. Benthic foraminiferal distribution over the last 5750 years
257 Fig. 5 shows percentages of the major species (> 5 %). Based on the distribution of these
258 dominant taxa, three different phases could be identified. The first phase does not map to the
259 environmental phases and ends at 2500 cal yr BP. During this phase (5750-2500 cal yr BP), *N.*
260 *scaphum* and *Ammonia beccarii* dominated, making up 30 and 18 % of the total species,
261 respectively. *Planorbulina mediterranensis* and *Bolivina spathulata* were relatively abundant
262 as well, with each ~10 % of the population. *A. beccarii* was particularly dominant (10-20 %)
263 between 5750 and 4750 cal yr BP and then quickly decreased to ~ 5 %. The epibenthic species
264 *Cibicides lobatulus* was only > 5 %, while *Hyalinea balthica* and *Uvigerina bifurcata* increased
265 until the end of the period. This first period was marked by a progressive increase of specific
266 richness; the S index increased from 28 to 36, and H' from 2.3 to 2.8. The foraminiferal density
267 (BFN) was relatively low during this period.
268 Between 2500 and 1250 cal yr BP, *Cassidulina carinata* increased sharply, while *N.*
269 *scaphum* clearly decreased in relative abundance. *Valvulineria bradyana* was nearly absent
270 during the first phase but became abundant from 2250 cal yr BP and reached 10 % of the fossil
271 assemblage during the latter period of this second phase. Smaller variation in the relative
272 abundances of the other dominant species, such as *P. mediterranea*, *A. beccarii*, *H. balthica*,
273 and *U. bifurcata*, was observed without a clear trend. *V. bradyana* and *Bulimina marginata*

increased, and *C. lobatulus* and *B. spathulata* diminished. The highest percentages of *C. carinata* (40 %) were observed between 1750 and 1500 BP, whereas *Bulimina marginata*, *P. mediterranensis*, and *B. spathulata* decreased. The BFN increased as both specific richness and the S index began an initial decline; specific richness was decreasing until 30 taxa, and H' until 2.5.

The last phase (1250 cal yr BP-present, Phase III) was characterized by higher relative abundance of *V. bradyana*, dominance of *C. carinata*, and a progressive decrease of *P. mediterranensis*, *A. beccarii*, and *B. spathulata.* The relative abundance of *N. scaphum* slightly increased from 1250 cal yr BP, compared to 2600-1250 cal yr BP, but decreased again from 500 cal yr BP. After 1000 cal yr BP, a strong increase was recorded for *C. carinata*, to more than 40 % at 500 cal yr BP and in the modern period. Deep infaunal species (i.e., *Chilostomella oolina* and *Globobulimina affinis*), *B. marginata*, and *Eggerelloides scaber* also increased during this phase. The last 200 years showed strong abundances of *C. carinata* (44 %) and a large loss of both *V. bradyana* and *N. scaphum*, which decreased to ~ 10 %. *Bolivina spathulata* and *H. balthica* totally disappeared, while *U. bifurcata*, *A. beccarii*, and *B. marginata* declined. With *C. carinata*, only *B. aculeata* and *E. scaber* are increasing during this modern period. The last 750 years showed a large decline of BFN, specific richness (~ 20), and S index (~ 2).

4.4. Multiproxy approach

A PCA was performed on the major environmental parameters (TOC, TN, $\delta^{13}C_{TOC}$, $\delta^{15}N_{bulk}$, BIT index, Ca/Ti, Fe/Ti, Br/Cl, Zr/Rb, and benthic foraminiferal stable isotopes) and on the relative abundances of the major benthic foraminiferal species (*C. carinata*, *N. scaphum*, *V. bradyana*, *A. beccarii*, *P. mediterranensis*, *B. spathulata*, *E. scaber*, *H. balthica*, *U. bifurcata*, *B. marginata*, and deep infaunas) (Fig. 6A). PC1 and PC2 explained 64 % (52 and 12 %, respectively) of the total variance observed in the dataset. The relative abundance of *N.*

299 *scaphum*, *A. beccarii*, and *P. mediterranensis* loaded positively on PC1 and negatively on PC2,
300 together with $\delta^{13}C_{bf}$, Ca/Ti, and Zr/Rb. Most organic compounds, such as TOC, TN, $\delta^{13}C_{TOC}$,
301 and $\delta^{15}N_{bulk}$, loaded negatively on PC1 and PC2 with *C. carinata*, Br/Cl, and Pb/Ti. The deep
302 infaunas and *B. marginata*, *V. bradyana*, and *E. scaber* loaded negatively on PC1 and positively
303 on PC2, together with Fe/Ti and the BIT index. *Uvigerina bifurcata*, *H. balthica*, and *B.*
304 *spatulata* loaded positively on PC1 and PC2 with $\delta^{18}O_{bf}$.

305 The scores of the different samples on PC1 and PC2 were plotted as a function of age
306 in Fig. 6B. The score of PC1 was stable during the first phase and then showed a slight increase
307 from 2500 to 2250 cal yr BP. At the start of Phase II (2250 cal yr BP), the score of PC1
308 decreased until 1500 cal yr BP, then increased again. At the start of Phase III (1250 cal yr BP),
309 a second progressive decrease started and characterized this phase until the present. The plot of
310 PC2 showed an increase toward positive loading until the end of phase I. The second phase
311 (2250-1250 cal yr BP) was characterized by a sharp decrease, before an increase at the
312 beginning of Phase III that continued until 750 cal yr BP. PC2 decreased, reaching 0 at 500 cal
313 yr BP, showed a slight increase between 500 and 250 cal yr BP, and decreased again during the
314 last period of Phase III.

315

316 **5. Discussion**

317 5.1. Benthic foraminiferal response to environmental and climatic changes

318 Climatic changes during the late Holocene have been well studied in the Portuguese
319 Margin, especially for the last 3000 years (e.g., Desprat et al., 2003; Abrantes et al., 2005;
320 Bartels-Jónsdóttir et al., 2006; Alt-Epping et al., 2009). This rendered the Holocene a suitable
321 period to test benthic foraminifera as bio-indicators for past Tagus River discharge and
322 environmental changes based on the living foraminiferal calibration developed by Dessandier
323 et al. (2016, 2018) in the same location. Previous sediment cores in the area extended back to

2000 (Abrantes et al., 2005; Bartels-Jónsdóttir et al., 2006) or 3000 cal yr BP (Alt-Epping et al., 2009). The 10-m core retrieved in our study provided a record that dated to 5750 cal yr BP. Next, we present the three phases defined by environmental changes related to sediment supplies, as shown by the XRF ratios and visible in the scores of the PCA (Fig. 6B).

The first phase was characterized by positive values of PC1 and a continuous increase in PC2, starting from negative values. The Zr/Rb ratio indicates a bigger grain size, which had a strong positive loading on PC1 together with Ca/Ti. Ca was previously linked to grain size in the Portuguese Margin and thought to be associated with coarse reworked shells of macrobenthic organisms (Martins et al., 2007; Abrantes et al., 2008; Alt-Epping et al., 2009). The two different increases of Zr/Rb and Ca/Ti were two successive phases in grain size decrease from Phase I to Phase III (Fig. 4). During Phase I, the TOC content of the sediment and the Br/Cl were very low; both indicated low amounts of organic compounds, likely because of this coarse grain size. This phase was characterized by river-influenced species, such as *N. scaphum*, *A. beccarii*, and *P. mediterranensis*. This first group of species consequently represents the river discharge bio-indicator in this study. Among them, *N. scaphum* was interpreted as an indicator of active upwelling conditions in previous studies of the Portuguese Margin (Bartels-Jónsdóttir et al., 2006). However, the results from late winter showed that this species was clearly dominant in the living community of the Portuguese inner shelf during winter. By contrast, during active upwelling context, it was present only in the dead community, reflecting lower relative abundances (Dessandier et al., 2016; 2018). The large occurrences of *A. beccarii* and *P. mediterranensis* during this first phase indicated strong bottom currents and coarse sediments (e.g., Murray, 2006; Schönfeld, 2002), whereas *C. lobatulus* was previously believed not to be endemic to this study area (Dessandier et al., 2018). The presence of the latter was probably an indicator of transport from the estuary to the shelf, as this species is typically found in Portuguese estuaries (Martins et al., 2015). The dominance of *N. scaphum* and *A.*

beccarii further suggested inputs from the estuary of phytoplankton or nutrients that may boost local marine productivity, such as coccolithophores, as has been previously observed where the Douro River flows into the ocean, where these species dominated the living fauna in late winter (Dessandier et al., 2015). This may indicate an influx of relatively labile organic matter, consistent with the progressive increase of faunal diversity during this period.

The second phase began with the Tagus mud belt establishment at around 2250 cal yr BP, which was represented by the plot of PC1, when the Ca/Ti and Zr/Rb counts clearly decreased and terrestrial elements (Fe/Ti, Pb/Ti, and BIT index, Fig. 4) increased. This suggests a deposition of finer sediments of terrestrial origin in the Tagus prodelta during this period. This important change in sedimentary conditions toward muddier and organic-rich sediment (Martins et al., 2006) was observed in the Portuguese Margin earlier, at around 2000 cal yr BP (Alt-Epping et al., 2009; Martins et al., 2007), and indicated the onset of the Tagus mud belt, which was mainly composed of sediment exported from the Tagus estuary (Jouanneau et al., 1998). This increase of organic compounds was also highlighted by the large increase in the Br/Cl ratio during this phase. The reduction of bottom water currents driven by decreasing wind and more humid conditions have been postulated as the physical processes that triggered a strong Tagus River export of sediment and led to the formation of the mud belt around this time (Alt-Epping et al., 2009). The mud belt formation was responsible for the increased accumulation of organic matter, especially during Phase II, corresponding to the increased levels of Br/Cl, TOC, and TN content (Fig. 4). The strong negative loading of both $\delta^{13}C_{TOC}$ and TOC on PC2 might suggest that the major supply of organic matter was driven by marine production, particularly during the strong upwelling conditions that characterized Phase II. The $\delta^{18}O_{bf}$ in this area was primarily controlled by salinity, with a reduced temperature effect, showing an increase in salinity during upwelling events (Lebreiro et al., 2006). This phase was characterized by a large increase of *C. carinata*, *V. bradyana*, and *B. marginata* abundances,

indicating that higher trophic levels occurred in the sediments, caused by high organic matter content in the mud belt. In this area, the active upwelling period corresponds to the most eutrophic conditions, mainly highlighted by the abundance of *C. carinata*, associated with marine organic matter (Br/Cl and $\delta^{13}C_{TOC}$; Fig. 6). *Cassidulina carinata* was already interpreted as highly dominant in an active upwelling context and adapted to cold, nutrient-rich waters (Bartels-Jónsdóttir et al., 2006; Martins et al., 2006). Together with this species, *V. bradyana, B. marginata, H. balthica*, and *U. bifurcate* have essentially been found only in the dead community and with almost no occurrence in the late winter (Dessandier et al., 2016). The increase in *V. bradyana* abundance correlated with the onset of Phase II and the mud belt. This result corroborated this species' need for rich trophic conditions and suggested that the second phase stabilized with the onset of strong upwelling conditions. *Nonion scaphum* and *V. bradyana* were highly dominant during this interval, although *N. scaphum* was less abundant than in Phase I. These two species live under organic-rich conditions and can tolerate anoxic sediments (Fontanier et al., 2002; Barras et al., 2014), which may suggest that large terrestrial inputs in this area led to periodic anoxia. The upwelling events create ideal environmental conditions for diatom blooms that resulted in the presence of other species during summer periods (Dessandier et al., 2016). This seasonal production indicated a preference of these opportunistic species for summer periods, when the influence of upwelling is at its maximum. During upwelling periods, diatoms are the major phytoplankton group responding to cold and nutrient-rich ENACW. However, the preservation of this group as fossils is dependent on high fluxes of individuals to the seabed (Abrantes et al., 1988), which constrains the use of this proxy for environmental changes. Conversely, winter periods characterized by maximum continental runoff had evidence of coccolithophore blooms, which responded to stratified waters (Abrantes and Moita, 1999). Since phytoplanktonic groups favor certain environmental conditions, these phytodetrital sources for benthic foraminifera may partially explain the seasonal variation in

399 species composition. This result may be the consequence of preferences for the specific
400 component of seasonally deposited phytodetritus, as has been observed in the Antarctic (Suhr
401 et al., 2003).

402 During Phases II and III, $\delta^{13}C_{bf}$, representing the exported phytodetritus to the seafloor
403 (Curry et al., 1988), indicated higher primary production, whereas the increase of $\delta^{15}N_{bulk}$ may
404 illustrate nutrient degradation or a stronger influence of estuarine sources of organic matter
405 (Owens, 1985). Phase III was characterized by a change in organic matter sources from
406 predominantly marine origin (negative loads on PC2) to predominantly terrestrial origin
407 (positive loads on PC2). This period showed a drop in foraminiferal diversity corresponding to
408 the dominance of *C. carinata* (up to 43 %). The increase in abundance of the deep infaunal
409 species at around 1000 cal yr BP suggested this is when the enrichment in organic matter of the
410 prodelta occurred and might indicate episodic periods of dysoxia or even anoxia related to
411 potential eutrophication, such as the occurrence of *G. affinis* and *C. oolina*, well known to live
412 in highly eutrophic conditions, often below the oxic sediments (Jorissen et al., 1998; Mojtahid
413 et al., 2010a). The faunal evolution, in terms of assemblages and diversity within Phases II and
414 III, revealed other controlling factors independent of the presence of the Tagus mud belt,
415 represented by the PC2 (Fig. 6B). An increase in pollutants during this period was thought to
416 occur concomitantly with the disappearance of *H. balthica* and appearance of *E. scaber*, as has
417 been observed off Iberian rivers (Diz et al., 2002; Bartels-Jónsdóttir et al., 2006). The increase
418 of pollutants indicated by the appearance of *E. scaber* also fits the results of Alve (1995), who
419 described *E. scaber* as a pollution-tolerant species under aquaculture influence.

420

421 5.2. Reconstruction of environmental evolution in the Tagus prodelta during the last 5750 years

422 5.2.1. First phase (5750-2250 cal yr BP): High Tagus River discharge

423 The modern sediment cover in the Tagus prodelta is mainly supplied by terrestrial silts
424 and clays exported by Tagus River discharge (Jouanneau et al., 1998). The influence of sea
425 level changes on the Iberian Margin is no longer significant on the sedimentation after ~ 7000
426 yr BP (Vis et al., 2008). The sedimentary evolution of the Tagus prodelta was mainly controlled
427 by Tagus River discharge and impacted by climatic changes after this period. This area was
428 particularly characterized by very humid conditions between 6500 and 5500 yr BP,
429 corresponding to the African Humid Period (deMenocal et al., 2000; Renssen et al., 2006; Vis
430 et al., 2010). The coarse sediments observed during Phase I, highlighted by both environmental
431 and faunal evidence, are in good agreement with conditions described by Rodrigues et al.
432 (2009), who interpreted intense deforestation and soil destabilization as factors responsible for
433 the increased current velocity of the Tagus River. These coarse sediments with low organic
434 content and of marine origin were similar to sediments of modern inner shelf conditions
435 observed down to 50 m water depth in the Portuguese Margin (Schmidt et al., 2010). These
436 conditions are synthesized in Fig. 7A and demonstrate that when the Tagus River discharge was
437 large, it prevented any deposition of fine material on the mud belt, resulting in low
438 sedimentation rates. The fine sediment deposits of terrestrial origin were probably transported
439 further offshore during this phase. The position of Core 64PE332-30-2 might have been a zone
440 of fine sediment bypass similar to what is currently observed on the inner shelf. This explains
441 the low organic content, the low BIT index, and the $\delta^{13}C_{TOC}$ that signaled the marine origin of
442 the sediments. Similar conditions were observed for this period in the Galicia mud deposit
443 (Martins et al., 2007; Bernárdez et al., 2008) and off the Guadiana River (Mendes et al., 2010)
444 and were believed to indicate a strong hydrodynamic regime. Tagus River floods have been
445 reconstructed in the lower Tagus River valley between 4900 and 3500 yr BP and were
446 associated with strong deforestation during this period (Vis et al., 2010).

447 The transition between Phases I and II was marked by a shift between the faunal and
448 environmental signals, between 2600 and 2250 cal yr BP (Fig. 5). The species that first reacted
449 to this, *C. carinata*, started to increase in abundance, resulting in a decrease in the relative
450 abundances of the other species, including the taxa indicators of river discharge. This reflected
451 the very opportunistic nature of *C. carinata* and provided a more accurate signal of the
452 environmental change than the geochemical parameters, which merely recorded the mud belt
453 conditions. A progressive decrease of fluvial influence was visible following the strong decline
454 of *A. beccarii* and *N. scaphum,* which has also been observed during the last 3000 years within
455 the Ría de Vigo (Diz et al., 2002). This may be the transition between colder and wetter
456 Subboreal conditions and warmer, dryer Sub-Atlantic conditions at 3000 yr BP (Alt-Epping et
457 al., 2009; Bernárdez et al., 2008). The Sub-Atlantic period was associated with the reduced
458 influence of winds on the Iberian Margin (Martins et al., 2007), a reduction in hydrodynamic
459 marine currents, and the collection of fine sediments in the Galicia mud deposit. These
460 conditions were responsible for the lateral movement of the mud deposit on the shelf, with the
461 construction of the mud belt at the beginning of Phase II (2250 cal yr BP). The accumulation
462 of muddy sediments on the shelf off the Tagus River at ~ 2000 years BP was synchronous with
463 the establishment of the mud belt off the Douro River (Drago et al., 1998). This coordination
464 suggests a response to regional rather than local change in the climate, responsible for a dryer
465 period and an increase of clay accumulation closer to the Tagus River mouth, due to the
466 decrease in Tagus discharge.
467
468 5.2.2. Second phase (2250-1250 cal yr BP): High upwelling intensity
469 After the onset of the Tagus mud belt at ~ 2250 cal yr BP, two alternative regimes
470 prevailed, one characterized by intense upwelling and the other by strong river discharge, as
471 summarized in Fig. 7B. During this phase, TN, $\delta^{13}C_{bf}$, and $\delta^{15}N_{bulk}$ showed an increase in

productivity, probably due to a change in Tagus River flux conditions. However, this was not recorded by all environmental parameters. The faunal results could indicate that the organic matter supply during Phase II was related to upwelling events more than Tagus River inputs. The decrease in the C/N ratio was not in agreement with $\delta^{13}C_{TOC}$ data, making it difficult to evaluate the organic matter source. The $\delta^{13}C_{TOC}$ and the C/N ratio are often used to determine the sources of organic matter (e.g., Hedges and Parker, 1976; Peters et al., 1978; Alt-Epping et al., 2007). However, the C/N ratio is affected by the preferential remineralization of nitrogen in marine sediments or nitrogen sorption onto clay minerals (Schubert and Calvert, 2001), and the $\delta^{13}C_{TOC}$ signal could be from a mixture of C3 and C4 plants, mimicking the isotopic signal of marine algae (e.g., Goñi et al., 1998). Both of these indicators in the paleorecords might be affected by organic matter degradation. Additionally, $\delta 15N_{bulk}$ could be affected in the study area by a higher influence of agriculture and pollution (Alt-Epping et al., 2009). Nevertheless, $\delta^{13}C_{TOC}$ and the C/N ratio were useful to discriminate the marine and terrestrial sources of organic matter in another study on the Portuguese Margin (Schmidt et al., 2010). In the present study, only the C/N ratio seemed to be clearly affected by the early diagenesis. These organic parameters were essential to compare the environmental signal with benthic foraminifera, and their disagreement confirms the importance of using a multiproxy approach that included bio-indicators that are less affected by organic matter degradation.

Phase II began at 2250 cal yr BP with a low amount of terrestrial input (indicated by the negative loading of PC2; Fig. 6) and lasted until 1800 cal yr BP, which corresponded to the RP (Lamb, 1985; Bernárdez et al., 2008). Despite the increase in eutrophy-tolerant species, the faunal diversity and BFN were low at the beginning of the RP. The deposition of contaminants and increased sediment accumulation rate may have limited faunal production during this period. Lebreiro et al. (2006) also observed a large export of terrestrial particles into the Tagus prodelta during the RP. This export was interpreted as a consequence of anthropogenic

activities, such as Roman gold mining, along the Tagus River. This export of terrestrial material may have been enhanced by the NAO- phase that occurred during that period and led to intensified rainfall in the Portuguese Margin (Abrantes et al., 2005). Periods of NAO- have strongly influenced Iberian river discharge, especially on the Tagus River (Trigo et al., 2004). The northern part of the Iberian Margin is marked by varying rainfall responses. This zone, which is very close to the limit of the NAO influence, is known to alternate between positive and negative correlation with the NAO and humid conditions (Alvarez and Gomez-Gesteira, 2006). Desprat et al. (2003) also identified warm and relatively humid conditions during the RP in the Ría de Vigo. A strong river regime such as this one was not observed off the Capbreton in the bay of Biscay (Mojtahid et al., 2009), suggesting an anti-correlation of the NAO phases between the two study areas.

The end of Phase II showed a decrease in the Tagus River influence that corresponded with an increase in positive loading of PC2, characterized by high marine organic matter content likely brought by active upwelling conditions. The increased abundance of *C. carinata* corroborated this context in the middle of Phase II, corresponding to a period of intense upwelling activity, which has also been described in the same area in a study using benthic foraminifera (Bartels-Jónsdóttir et al., 2006). The dominance of the opportunistic species *C. carinata* constrained faunal diversity, as observed in other studies (Fontanier et al., 2003; Dessandier et al., 2018). However, *C. carinata* did not increase until the end of Phase II, suggesting that the intensity of upwelling slowed down at the end of this phase. By contrast, the Tagus mud belt built up, allowing an increased deposition of marine organic matter until the end of Phase II. This difference could be the result of biased organic parameters (e.g., caused by early diagenesis). In addition, this study area was characterized by organic matter from different sources, which were recorded as a mixture of marine and terrestrial compounds by the organic parameters. What was revealed by the organic parameters as a record of upwelling

activity could instead result from high productivity throughout the entire year. Therefore, benthic foraminiferal species recorded the organic matter sources more accurately.

5.2.3. Third phase (1250 cal yr BP-present): Alternating upwelling and Tagus discharge influence

The beginning of Phase III (Fig. 7C), which corresponds to the DA, was followed by the MWP, which occurred between 1100 and 600 yr BP, as reported in several studies performed on the Portuguese Margin (e.g., Desprat et al., 2003; Rosa et al., 2007). The DA was described as a period characterized by strong upwelling activity off the Douro River (Rosa et al., 2007). The MWP is also well known in the Portuguese Margin as a period characterized by active upwelling conditions triggered by NAO+ conditions (Abrantes et al., 2005; Bartels-Jónsdóttir et al., 2006; Rosa et al., 2007; Rodrigues et al., 2009). The high primary productivity was linked to upwelling events and created eutrophic conditions in sediments that allowed for less competition among *B. spathulata*, *P. mediterranensis*, *Cribroelphidium gerthi*, and *H. balthica*. This period, characterized by a warm and dry climate, was influenced by anthropogenic activities and soil erosion (Rodrigues et al., 2009) that caused Fe and Pb to be massively transported via Tagus River runoff to the prodelta. Dry soils restrained infiltration and possibly triggered large flooding of the Tagus River (Benito et al., 2003). The increased BIT index (Warden et al., 2016) and Fe/Ti and Pb/Ti ratios during the beginning of the MWP suggested increased terrestrial input, corresponding with the increased loading of PC2 in the first part of Phase III and the accumulation of finer sediments.

The LIA, between 600 and 100 yr BP, was characterized by the increase in terrestrial material, as shown by the abrupt increase in the BIT index and Fe/Ti and Pb/Ti ratios at 250 cal yr BP. This increase was also highlighted by the sharp decrease in PC2 (Fig. 6B), which could be linked to the Lisbon earthquake in 1755 AD (200 cal yr BP; Abrantes et al., 2008) or to

547 massive exports of fine sediments from the Tagus River (low Zr/Rb). This period has been
548 described as characterized by abrupt cooling and wet conditions (Bradley, 2000). The LIA was
549 affected by high-frequency episodic Tagus River paleo-floods (Benito et al., 2003) and has been
550 associated with the transport of fine sediments from the continent via discharge from the Tagus
551 River under NAO- conditions (Abrantes et al., 2005; Bartels-Jónsdóttir et al., 2006). During the
552 LIA, an abrupt decrease in the abundance of *C. carinata* may indicate that a reduction in
553 upwelling conditions occurred. *V. bradyana*, *E. scaber*, *A. beccarii*, and deep infaunas
554 increased, possibly as a consequence of episodic anoxia and the presence of contaminants. The
555 presence of the deep infaunas that can tolerate refractory organic matter (Murray, 2006)
556 suggests a decrease in organic matter quality, as was also observed in the Galicia mud deposit
557 during this period (Martins et al., 2006). This decrease in quality may be the major cause of the
558 decreased infaunal diversity that occurred between 1000 cal yr BP and the present.
559 Nevertheless, the faunal results suggested that intense upwelling periods also occurred during
560 the LIA, as demonstrated by the increased abundance of *C. carinata*. This highlighted that this
561 period was unstable and characterized by several environmental changes. The results from this
562 study were in good agreement with previous studies in the same area for the last 2000 years
563 (Abrantes et al., 2005; Bartels-Jónsdóttir et al., 2006; Alt-Epping et al., 2009), except for small
564 time shifts in the upwelling versus Tagus River discharge periods corresponding to the
565 transition between Phases I and II. These time shifts could be the consequence of different age
566 models. Bartels-Jónsdóttir et al. (2006) demonstrated that an "intense upwelling period"
567 occurred, followed by a "very intense upwelling period" during the MWP, and finally a large
568 Tagus River discharge during the LIA, all determined through the analysis of benthic
569 foraminiferal distribution.

570 There were some differences during the MWP and the LIA between the reconstructions
571 from this study and the results from Bartels-Jónsdóttir et al. (2006). These variations could be

572 due to a different interpretation of certain species, specifically *N. scaphum*, which was
573 determined to be controlled by upwelling in previous studies; by contrast, it was used as a river
574 discharge proxy in this study, based on the ecological results from the study area (Dessandier
575 et al., 2016). The use of environmental data combined with the composition of the major species
576 in this study may allow a better interpretation of the mud belt onset than merely using benthic
577 foraminiferal data. Our results were also in good agreement with the reconstruction of the Tagus
578 River discharge and the upwelling strength reported in Abrantes et al. (2009).

579 Finally, during the last century, this area was contaminated by anthropogenic pollution,
580 including numerous trace metals that were measured in excess in the Tagus estuary, such as
581 AS, Pb, Zn, Cu, and Cd (Caçador et al., 1996; Jouanneau et al., 1998). The catchment area was
582 also influenced by anthropogenic contaminants, such as domestic sewage and industrial wastes
583 (e.g., petrochemistry, fertilizers, smelters; Carvalho, 1997). Our analyses were not performed
584 to identify the sources of anthropogenic pollution; however, the XRF signal shows a clear
585 increase of several contaminants (such as Pb) in the most recent interval. We do not have
586 enough faunal resolution and environmental data to investigate the anthropogenic influence on
587 benthic ecosystems, but we assume that the faunal assemblages respond to this anthropogenic
588 activity, as shown in other environments (e.g., Alve, 1995). The faunal distribution shows
589 increased abundances of deep infaunal species and of *E. scaber* but the disappearance of other
590 species, such as *H. balthica*, as has already been observed as a consequence of anthropogenic
591 pollution in the Tagus prodelta (Bartels-Jónsdóttir et al., 2006). The last century was also
592 characterized by the construction of dams, which have likely influenced the sequestration of
593 organic matter in the estuary and changed the influence of the Tagus River discharge on the
594 shelf through increased input of finer material (Jouanneau et al., 1998) and increased correlation
595 with NAO phases (Trigo et al., 2004), all of which could have significant environmental
596 consequences that will be crucial to understand in the future.

6. Conclusions

The results of this study demonstrate the validity of using benthic foraminifera as bio-indicators of past river discharge and upwelling intensity in the Tagus prodelta during the last 5750 years. Major environmental changes, linked with late Holocene climatic variations, are summarized by key benthic foraminiferal taxa data in Fig. 8. This study showed an additional phase, between 5750 and 2250 cal yr BP, that has not yet been investigated in the Portuguese shelf. This phase was characterized by coarser sediment cover and dominated mostly by *N. scaphum* and *A. beccarii*, suggesting a very dynamic Tagus River system that facilitated the dispersion of coarse terrigenous particles onto the prodelta.

The progressive decrease of the Tagus River flow, resulting in the establishment of the modern Tagus mud belt, was the major process explaining the environmental changes that occurred before Phase II. The presence of a transition period (2500-2250 cal yr BP) at the end of Phase I was only supported by the composition of the benthic foraminifera; geochemical data did not reveal any environmental changes. This might be due to the extremely poor preservation of organic matter in coarse sediments (in which benthic foraminifera are fairly well preserved).

Phase II (2250-1250 cal yr BP) was characterized by fine continental deposits, responsible for a better food stock for benthic organisms throughout the record. This phase was marked by the increase of *C. carinata*, *V. bradyana*, and *B. marginata*, opportunistic species that mark the increase in upwelling intensity in this area, revealing the strongest upwelling activity during the DA and the MWP. The high organic matter stocks in the Tagus prodelta during this phase created more refractory organic matter, responsible for a faunal diversity decrease from 2250 cal yr BP to present.

Phase III (1250 cal yr BP-present) showed the disappearance of *B. spathulata*, *P. mediterranensis*, and *H. balthica* and the decrease of *A. beccarii* and *N. scaphum*, which may

be a consequence of a decrease in the organic matter quality and/or the occurrence of anthropogenic pollution, as indicated by benthic foraminiferal assemblages and the XRF data. Conversely, *E. scaber* increased, probably because of its pollution tolerance, and *C. carinata* remained dominant, likely due to the strong upwelling conditions. Benthic foraminifera responded accurately to record environmental and climate changes in the North Atlantic continental shelf and therefore could be used as a bio-indicator of environmental changes, such as changes in upwelling activity and river discharge, that were directly linked with the NAO.

Acknowledgments

The authors wish to thank the captain and crew of R/V *Pelagia* and NIOZ marine technicians for work at sea and Silvia Nave at LNEG for the help during the cruise preparation. Ship time for R/V *Pelagia* cruise 64PE332 was funded by the Netherlands Organization for Scientific Research (NWO), as part of the PACEMAKER project, funded by the ERC under the European Union's Seventh Framework Program (FP7/2007-2013). Part of the radiocarbon analyses were funded by the HAMOC (ANR) Project. J.-H. Kim was also partly supported by the National Research Foundation of Korea (NRF) grant funded by the Korea government (MSICT) (No. NRF-2016R1A2B3015388, PN17100). P.-A. Dessandier was supported by the Research Council of Norway through its Center of Excellence funding scheme for CAGE, project number 223259.

References

Abrantes, F., 1988. Diatom assemblages as upwelling indicators in surface sediments off Portugal. Mar. Geol. 85, 15–39.Abrantes, F., Moita, M.T., 1999. Water column and

recent sediment data on diatoms and coccolithophorids, off Portugal, confirm sediment record of upwelling events. Oceanologica Acta 22, 67–84.

Abrantes, F., Lebreiro, S., Rodrigues, T., Gil, I., Bartels-Jónsdóttir, H., Oliveira, P., Kissel, C., Grimalt, J.O., 2005. Shallow-marine sediment cores record climate variability and earthquake activity off Lisbon (Portugal) for the last 2000 years. Quaternary Science Reviews 24, 2477–2494.

Abrantes, F., Alt-Epping, U., Lebreiro, S., Voelker, A., Schneider, R., 2008. Sedimentological record of tsunamis on shallow-shelf areas: The case of the 1969 AD and 1755 AD tsunamis on the Portuguese Shelf off Lisbon. Marine Geology 249, 283–293.

Aguiar, F.C., Ferreira, M.T., 2005. Human-disturbed landscapes: effects on composition and integrity of riparian woody vegetation in the Tagus River basin, Portugal. Environmental Conservation 32, 30–41.

Alt-Epping, U., Mil-Homens, M., Hebbeln, D., Abrantes, F., Schneider, R.R., 2007. Provenance of organic matter and nutrient conditions on a river-and upwelling influenced shelf: a case study from the Portuguese Margin. Marine Geology 243, 169–179.

Alt-Epping, U., Stuut, J.-B.W., Hebbeln, D., Schneider, R., 2009. Variations in sediment provenance during the past 3000 years off the Tagus River, Portugal. Marine Geology 261, 82–91.

Alvarez, I., Gomez-Gesteira, M., 2006. Influence of teleconnection patterns on precipitation variability and on river flow regimes in the Miño River basin (NW Iberian Peninsula). Clim Res 32, 63–73.

Alve, E., 1995. Benthic foraminiferal responses to estuarine pollution: a review. Journal of Foraminiferal Research 25, 190–203.

670 Azevedo, I.C., Duarte, P.M., Bordalo, A.A., 2008. Understanding spatial and temporal
671 dynamics of key environmental characteristics in a mesotidal Atlantic estuary (Douro,
672 NW Portugal). Estuarine, Coastal and Shelf Science 76, 620–633.
673 Barras, C., Jorissen, F.J., Labrune, C., Andral, B., Boissery, P., 2014. Live benthic foraminiferal
674 faunas from the French Mediterranean Coast: towards a new biotic index of
675 environmental quality. Ecological Indicators 36, 719–743.
676 Bartels-Jónsdóttir, H.B., Knudsen, K.L., Abrantes, F., Lebreiro, S., Eiríksson, J., 2006. Climate
677 variability during the last 2000 years in the Tagus Prodelta, western Iberian Margin:
678 Benthic foraminifera and stable isotopes. Marine Micropaleontology 59, 83–103.
679 Benito, G., Sopeña, A., Sánchez-Moya, Y., Machado, M.J., Pérez-González, A., 2003.
680 Palaeoflood record of the Tagus River (central Spain) during the Late Pleistocene and
681 Holocene. Quaternary Science Reviews 22, 1737–1756.
682 Bernárdez, P., González-Álvarez, R., Francés, G., Prego, R., Bárcena, M.A., Romero, O.E.,
683 2008. Late Holocene history of the rainfall in the NW Iberian peninsula—Evidence
684 from a marine record. Journal of Marine Systems 72, 366–382.
685 Bond, G., Showers, W., Cheseby, M., Lotti, R., Almasi, P., Priore, P., Cullen, H., Hajdas, I.,
686 Bonani, G., 1997. A pervasive millennial-scale cycle in North Atlantic Holocene and
687 glacial climates. Science 278, 1257–1266.
688 Bradley, R.S., 2000. Enhanced: 1000 years of climate change. Science 288, 1353–1355.
689 Caçador, I., Vale, C., Catarino, F., 1996. Accumulation of Zn, Pb, Cu, Cr and Ni in sediments
690 between roots of the Tagus estuary salt marshes, Portugal. Estuarine, Coastal and Shelf
691 Science 42, 393–403.
692 Carvalho, F.P., 1997. Distribution, cycling and mean residence time of ^{226}Ra, ^{210}Pb and^{210}Po in
693 the Tagus estuary. Science of the total environment 196, 151–161.

694 Curry, W.B., Duplessy, J.-C., Labeyrie, L.D., Shackleton, N.J., 1988. Changes in the
695 distribution of δ13C of deep water ΣCO2 between the last glaciation and the Holocene.
696 Paleoceanography 3, 317–341.
697 Clarke, K. R., and R. M. Warwick (1994), Change in Marine Communities: An Approach to
698 Statistical Analysis and Interpretation, PRIMER-E Ltd.
699 Desprat, S., Sánchez Goñi, M.F., Loutre, M.-F., 2003. Revealing climatic variability of the last
700 three millennia in northwestern Iberia using pollen influx data. Earth and Planetary
701 Science Letters 213, 63–78.
702 Dessandier, P.-A., Bonnin, J., Kim, J.-H., Bichon, S., Grémare, A., Deflandre, B., de Stigter,
703 H., Malaizé, B., 2015. Lateral and vertical distributions of living benthic foraminifera
704 off the Douro River (western Iberian margin): Impact of the organic matter quality.
705 Marine Micropaleontology 120, 31–45.
706 Dessandier, P.-A., Bonnin, J., Kim, J.-H., Bichon, S., Deflandre, B., Grémare, A., Sinninghe
707 Damsté, J.S., 2016. Impact of organic matter source and quality on living benthic
708 foraminiferal distribution on a river-dominated continental margin: A study of the
709 Portuguese Margin. Journal of Geophysical Research: Biogeosciences 121, 1689–1714.
710 Dessandier, P.-A., Bonnin, J., Kim, J.-H., Racine, C., 2018. Comparison of living and dead
711 benthic foraminifera on the Portuguese Margin: understanding the taphonomical
712 processes. Marine micropaleontology 140, 1–16.
713 Dias, J.M.A., Jouanneau, J.M., Gonzalez, R., Araújo, M.F., Drago, T., Garcia, C., Oliveira, A.,
714 Rodrigues, A., Vitorino, J., Weber, O., 2002. Present day sedimentary processes on the
715 northern Iberian shelf. Progress in Oceanography 52, 249–259.
716 Diz, P., Francés, G., Pelejero, C., Grimalt, J.O., Vilas, F., 2002. The last 3000 years in the Ría
717 de Vigo (NW Iberian Margin): climatic and hydrographic signals. The Holocene 12,
718 459–468.

719 Drago, T., Oliveira, A., Magalhães, F., Cascalho, J., Jouanneau, J.-M., Vitorino, J., 1998. Some
720 evidences of northward fine sediment transport in the northern Portuguese continental
721 shelf. Oceanologica Acta 21, 223–231.
722 Ferreira, J.G., Duarte, P., 1994. Productivity of the Tagus estuary: an application of the EcoWin
723 ecological model. Gaia 8, 89–95.
724 Fiúza, A.F., 1983. Upwelling patterns off Portugal, in: Coastal Upwelling Its Sediment Record.
725 Springer, pp. 85–98.
726 Fontanier, C., Jorissen, F.J., Licari, L., Alexandre, A., Anschutz, P., Carbonel, P., 2002. Live
727 benthic foraminiferal faunas from the Bay of Biscay: faunal density, composition, and
728 microhabitats. Deep Sea Research Part I: Oceanographic Research Papers 49, 751–785.
729 Fontanier, C., Jorissen, F.J., Chaillou, G., David, C., Anschutz, P., Lafon, V., 2003. Seasonal
730 and interannual variability of benthic foraminiferal faunas at 550m depth in the Bay of
731 Biscay. Deep Sea Research Part I: Oceanographic Research Papers 50, 457–494.
732 Fontanier, C., Jorissen, F.J., Chaillou, G., Anschutz, P., Grémare, A., Griveaud, C., 2005. Live
733 foraminiferal faunas from a 2800m deep lower canyon station from the Bay of Biscay:
734 faunal response to focusing of refractory organic matter. Deep Sea Research Part I:
735 Oceanographic Research Papers 52, 1189–1227.
736 Frouin, R., Fiúza, A.F.G., Ambar, I., Boyd, T.J., 1990. Observations of a poleward surface
737 current off the coasts of Portugal and Spain during winter. Journal of Geophysical
738 Research 95, 679. doi:10.1029/JC095iC01p00679
739 Goineau, A., Fontanier, C., Jorissen, F.J., Lansard, B., Buscail, R., Mouret, A., Kerhervé, P.,
740 Zaragosi, S., Ernoult, E., Artéro, C., 2011. Live (stained) benthic foraminifera from the
741 Rhône prodelta (Gulf of Lion, NW Mediterranean): Environmental controls on a river-
742 dominated shelf. Journal of Sea Research 65, 58–75.

743 Goldstein, S.T., Corliss, B.H., 1994. Deposit feeding in selected deep-sea and shallow-water
744 benthic foraminifera. Deep Sea Research Part I: Oceanographic Research Papers 41,
745 229–241.
746 Goñi, M.A., Ruttenberg, K.C., Eglinton, T.I., 1998. A reassessment of the sources and
747 importance of land-derived organic matter in surface sediments from the Gulf of
748 Mexico. Geochimica et Cosmochimica Acta 62, 3055–3075.
749 Hammer, Ø., Harper, D.A.T., Ryan, P.D., 2001. Past: Paleontological Statistics Software
750 Package for education and data analysis. Paleontología Electrónica 4: 1-9. URL:<
751 http://palaeo-electronica. org/2001_1/past/issue1_01. html.
752 Hedges, J.I., Parker, P.L., 1976. Land-derived organic matter in surface sediments from the
753 Gulf of Mexico. Geochimica et Cosmochimica Acta 40, 1019–1029.
754 Jorissen, F.J., de Stigter, H.C., Widmark, J.G., 1995. A conceptual model explaining benthic
755 foraminiferal microhabitats. Marine Micropaleontology 26, 3–15.
756 Jorissen, F.J., Wittling, I., Peypouquet, J.P., Rabouille, C., Relexans, J.C., 1998. Live benthic
757 foraminiferal faunas off Cape Blanc, NW-Africa: community structure and
758 microhabitats. Deep-Sea Research Part I 45, 2157–2188.
759 Jorissen, F.J., Fontanier, C., Thomas, E., 2007. Paleoceanographical proxies based on deep-sea
760 benthic foraminiferal assemblage characteristics. Proxies in Late Cenozoic
761 Paleoceanography, Dev. Mar. Geol 1, 263–325.
762 Jouanneau, J.M., Garcia, C., Oliveira, A., Rodrigues, A., Dias, J.A., Weber, O., 1998. Dispersal
763 and deposition of suspended sediment on the shelf off the Tagus and Sado estuaries, SW
764 Portugal. Progress in Oceanography 42, 233–257.
765 Keigwin, L.D., Pickart, R.S., 1999. Slope water current over the Laurentian Fan on interannual
766 to millennial time scales. Science 286, 520–523.

767 Kitazato, H., Shirayama, Y., Nakatsuka, T., Fujiwara, S., Shimanaga, M., Kato, Y., Okada, Y.,
768 Kanda, J., Yamaoka, A., Masuzawa, T., Suzuki, K., 2000. Seasonal phytodetritus
769 deposition and responses of bathyal benthic foraminiferal populations in Sagami Bay,
770 Japan: preliminary results from "Project Sagami 1996–1999." Marine
771 Micropaleontology 40, 135–149.
772 Lamb, H.H., 1985. An approach to the study of the development of climate and its impact in
773 human affairs. Climate and History: Studies in Past Climates and Their Impact on Man
774 291–309.
775 Lebreiro, S.M., Francés, G., Abrantes, F.F.G., Diz, P., Bartels-Jónsdóttir, H.B., Stroynowski,
776 Z.N., Gil, I.M., Pena, L.D., Rodrigues, T., Jones, P.D., Nombela, M.A., Alejo, I., Briffa,
777 K.R., Harris, I., Grimalt, J.O., 2006. Climate change and coastal hydrographic response
778 along the Atlantic Iberian margin (Tagus Prodelta and Muros Ría) during the last two
779 millennia. The Holocene 16, 1003–1015.
780 Martins, M.V.A., Jouanneau, J.-M., Weber, O., Rocha, F., 2006. Tracing the late Holocene
781 evolution of the NW Iberian upwelling system. Marine Micropaleontology 59, 35–55.
782 Martins, M.V.A., Dubert, J., Jouanneau, J.-M., Weber, O., da Silva, E.F., Patinha, C., Dias,
783 J.M.A., Rocha, F., 2007. A multiproxy approach of the Holocene evolution of shelf–
784 slope circulation on the NW Iberian Continental Shelf. Marine Geology 239, 1–18.
785 Martins, M.V.A., Silva, F., Laut, L.M., Frontalini, F., Clemente, I., Miranda, P., Figueira, R.,
786 Sousa, S.H., Dias, J.M.A., 2015. Response of benthic foraminifera to organic matter
787 quantity and quality and bioavailable concentrations of metals in Aveiro Lagoon
788 (Portugal). Plos One. Doi: PONE-D-14-38075R1.
789 Mayewski, P.A., Rohling, E.E., Stager, J.C., Karlén, W., Maasch, K.A., Meeker, L.D.,
790 Meyerson, E.A., Gasse, F., van Kreveld, S., Holmgren, K., Lee-Thorp, J., Rosqvist, R.,

Rack, F., Staubwasser, M., Schneider, R.R., Steig, E.J., 2004. Holocene climate variability. Quaternary Research 62, 243–255.

McCave, I.N., Hall, I.R., 2002. Turbidity of waters over the Northwest Iberian continental margin. Progress in Oceanography 52, 299–313.

Mendes, I., Gonzalez, R., Dias, J.M.A., Lobo, F., Martins, V., 2004. Factors influencing recent benthic foraminifera distribution on the Guadiana shelf (Southwestern Iberia). Marine Micropaleontology 51, 171–192.

Mendes, I., Rosa, F., Dias, J.A., Schönfeld, J., Ferreira, Ó., Pinheiro, J., 2010. Inner shelf paleoenvironmental evolution as a function of land–ocean interact ions in the vicinity of the Guadiana River, SW Iberia. Quaternary International 221, 58–67.

Mendes, I., Dias, J.A., Schönfeld, J., Ferreira, Ó., 2012. Distribution of living benthic foraminifera on the northern Gulf of Cadiz continental shelf. The Journal of Foraminiferal Research 42, 18–38.

Mojtahid, M., Jorissen, F., Lansard, B., Fontanier, C., Bombled, B., Rabouille, C., 2009. Spatial distribution of live benthic foraminifera in the Rhône prodelta: Faunal response to a continental–marine organic matter gradient. Marine Micropaleontology 70, 177–200.

Mojtahid, M., Griveaud, C., Fontanier, C., Anschutz, P., Jorissen, F.J., 2010a. Live benthic foraminiferal faunas along a bathymetrical transect (140–4800m) in the Bay of Biscay (NE Atlantic). Revue de micropaléontologie 53, 139–162.

Mojtahid, M., Jorissen, F., Lansard, B., Fontanier, C., 2010b. Microhabitat selection of benthic foraminifera in sediments off the Rhône River mouth (NW Mediterranean). The Journal of Foraminiferal Research 40, 231–246.

Murray, J.W., 2006. Ecology and applications of benthic foraminifera. Cambridge University Press.

Oliveira, A., Santos, A.I., Rodrigues, A., Vitorino, J., 2007. Sedimentary particle distribution and dynamics on the Nazaré canyon system and adjacent shelf (Portugal). Marine Geology 246, 105–122.

Ortega, P., Lehner, F., Swingedouw, D., Masson-Delmotte, V., Raible, C.C., Casado, M., Yiou, P., 2015. A model-tested North Atlantic Oscillation reconstruction for the past millennium. Nature 523, 71–74.

Owens, N.J.P., 1985. Variations in the natural abundance of 15 N in estuarine suspended particulate matter: a specific indicator of biological processing. Estuarine, Coastal and Shelf Science 20, 505–510.

Peliz, Á., Rosa, T.L., Santos, A.M.P., Pissarra, J.L., 2002. Fronts, jets, and counter-flows in the Western Iberian upwelling system. Journal of Marine Systems 35, 61–77.

Peters, K.E., Sweeney, R.E., Kaplan, I.R., 1978. Correlation of carbon and nitrogen stable isotope ratios in sedimentary organic matter 1. Limnology and Oceanography 23, 598–604.

Prieto, L., Navarro, G., Rodríguez-Gálvez, S., Huertas, I.E., Naranjo, J.M., Ruiz, J., 2009. Oceanographic and meteorological forcing of the pelagic ecosystem on the Gulf of Cadiz shelf (SW Iberian Peninsula). Continental Shelf Research 29, 2122–2137.

Relvas, P., Barton, E.D., Dubert, J., Oliveira, P.B., Peliz, A., Da Silva, J.C.B., Santos, A.M.P., 2007. Physical oceanography of the western Iberia ecosystem: latest views and challenges. Progress in Oceanography 74, 149–173.

Rodrigues, T., Grimalt, J.O., Abrantes, F.G., Flores, J.A., Lebreiro, S.M., 2009. Holocene interdependences of changes in sea surface temperature, productivity, and fluvial inputs in the Iberian continental shelf (Tagus mud patch). Geochemistry, Geophysics, Geosystems 10.

839 Rosa, F., Fatela, F., Drago, T., 2007. Late Holocene benthic foraminiferal records in the
840 continental shelf off Douro River (NW Portugal): evidences for productivity and
841 sedimentary relationships. Thalassas 23, 19–31.
842 Schmidt, F., Hinrichs, K.-U., Elvert, M., 2010. Sources, transport, and partitioning of organic
843 matter at a highly dynamic continental margin. Marine Chemistry 118, 37–55.
844 Schönfeld, J., 2002. A new benthic foraminiferal proxy for near-bottom current velocities in
845 the Gulf of Cadiz, northeastern Atlantic Ocean. Deep Sea Research Part I:
846 Oceanographic Research Papers 49, 1853–1875.
847 Schubert, C.J., Calvert, S.E., 2001. Nitrogen and carbon isotopic composition of marine and
848 terrestrial organic matter in Arctic Ocean sediments:: implications for nutrient
849 utilization and organic matter composition. Deep Sea Research Part I: Oceanographic
850 Research Papers 48, 789–810.
851 Stuiver, M., Reimer, J., 1993. Extended 14C data base and revised CALIB 3.014 C age
852 calibration program. EDITORIAL COMMENT 35, 215–230.
853 Stuut, J.-B.W., Temmesfeld, F., De Deckker, P., 2014. A 550 ka record of aeolian activity near
854 North West Cape, Australia: inferences from grain-size distributions and bulk chemistry
855 of SE Indian Ocean deep-sea sediments. Quaternary Science Reviews 83, 83–94.
856 Suhr, S.B., Pond, D.W., Gooday, A.J., Smith, C.R., 2003. Selective feeding by benthic
857 foraminifera on phytodetritus on the western Antarctic Peninsula shelf: evidence from
858 fatty acid biomarker analysis. Marine Ecology Progress Series 262, 153–162.
859 Swingedouw, D., Ortega, P., Mignot, J., Guilyardi, E., Masson-Delmotte, V., Butler, P.G.,
860 Khodri, M., Séférian, R., 2015. Bidecadal North Atlantic ocean circulation variability
861 controlled by timing of volcanic eruptions. Nature communications 6.
862 Taylor, S.R., 1965. The application of trace element data to problems in petrology. Phys. Chem.
863 Earth 6, 133–213.

Tilstone, G.H., Figueiras, F.G., Lorenzo, L.M., Arbones, B., 2003. Phytoplankton composition, photosynthesis and primary production during different hydrographic conditions at the Northwest Iberian upwelling system. Marine Ecology Progress Series 252, 89–104.

Tjallingii, R., Röhl, U., Kölling, M., Bickert, T., 2007. Influence of the water content on X-ray fluorescence core-scanning measurements in soft marine sediments. Geochemistry, Geophysics, Geosystems 8.

Trigo, R.M., Pozo-Vàzquez, D., Osborn T.J., Castro-Díez, Y., Gámiz-Fortis, S., Esteban-Parra, M.J., 2004. North Atlantic Oscillation influence on precipitation, river flow and water resources in the Iberian Peninsula. International Journal Of Climatology 24, 925–944.

Trouet, V., Esper, J., Graham, N.E., Baker, A., Scourse, J.D., Frank, D.C., 2009. Persistent positive North Atlantic Oscillation mode dominated the medieval climate anomaly. Science 324, 78–80.

Vale, C., Sundby, B., 1987. Suspended sediment fluctuations in the Tagus estuary on semi-diurnal and fortnightly time scales. Estuarine, Coastal and Shelf Science 25, 495–508.

van Aken, H.M., 2000a. The hydrography of the mid-latitude northeast Atlantic Ocean: I: The deep water masses. Deep Sea Research Part I: Oceanographic Research Papers 47, 757–788.

van Aken, H.M., 2000b. The hydrography of the mid-latitude Northeast Atlantic Ocean: II: The intermediate water masses. Deep Sea Research Part I: Oceanographic Research Papers 47, 789–824.

Vitorino, J., Oliveira, A., Jouanneau, J.M., Drago, T., 2002a. Winter dynamics on the northern Portuguese shelf. Part 2: bottom boundary layers and sediment dispersal. Progress in Oceanography 52, 155–170.

Vitorino, J., Oliveira, A., Jouanneau, J.M., Drago, T., 2002b. Winter dynamics on the northern Portuguese shelf. Part 1: physical processes. Progress in Oceanography 52, 129–153.

Wanner, H., Brönniman, S., Casty, C., Gyalistras, D., Luterbacher, J., Schmutz, C., Stephenson, D.B., Xoplaki, E., 2001. North Atlantic Oscillation – concept and studies. Surveys in Geophysics 22, 321–381.

Warden, L., Kim, J.-H., Zell, C., Vis, G.-J., de Stigter, H., Bonnin, J., Damsté, J.S.S., 2016. Examining the provenance of branched GDGTs in the Tagus River drainage basin and its outflow into the Atlantic Ocean over the Holocene to determine their usefulness for paleoclimate applications. Biogeosciences 13, 5719-5738.

Weltje, G.J., Tjallingii., R, 2008. Calibration of XRF core scanners for quantitative geochemical logginig of sediment cores: Theory and application. Earth and Planetary Science Letters274, 423-438.

Ziegler, M., Jilbert, T., de Lange, G.J., Lourens, L.J., Reichart, G.-J., 2008. Bromine counts from XRF scanning as an estimate of the marine organic carbon content of sediment cores. Geochemistry. Geophysics. Geosystems 9.

Figures

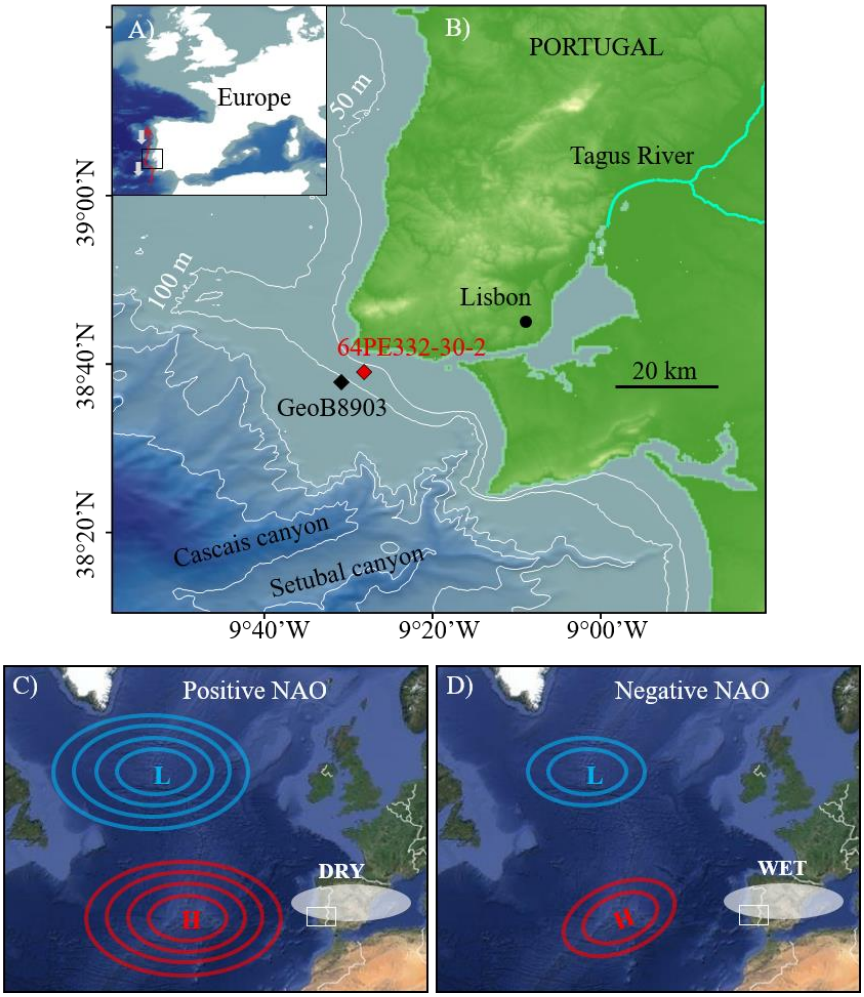

Fig. 1. A) General location map of the study area, with a schematic representation of the Portugal Coastal Counter Current (red arrow) and the ENACW (grey arrows). B) Detailed map of the core locations considered in this study. Red diamond: piston cores 64PE332-30-2, this study; black diamond: GeoB8903 (Abrantes et al., 2008). C) Positive and D) Negative phase of NAO with L = Iceland low-pressure system and H = Azores high-pressure system.

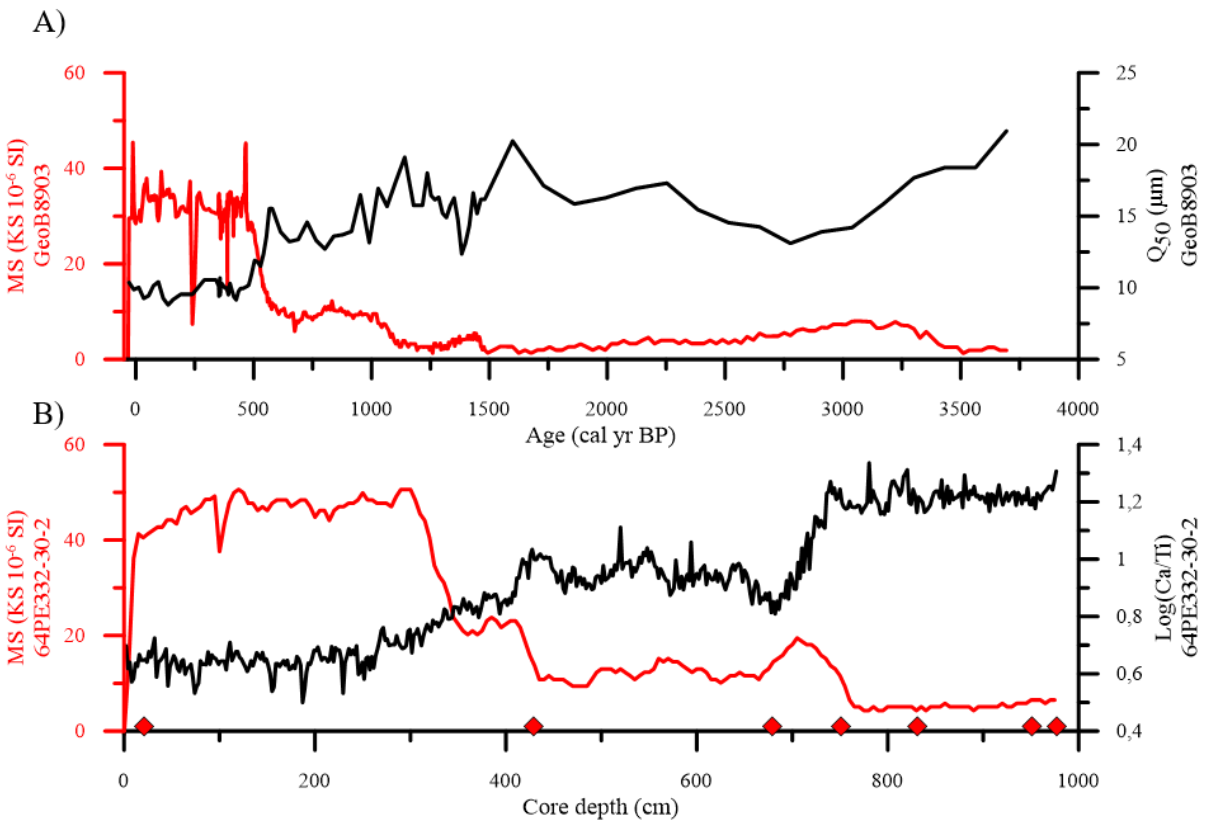

Fig. 2. Comparison of Ca/Ti and magnetic susceptibility (MS) of Core 64PE332-30-2 with grain size (Q_{50}) and MS from Core GeoB 8903 (Abrantes et al., 2008; Alt-Epping et al., 2009). Red diamonds represent ^{14}C data points.

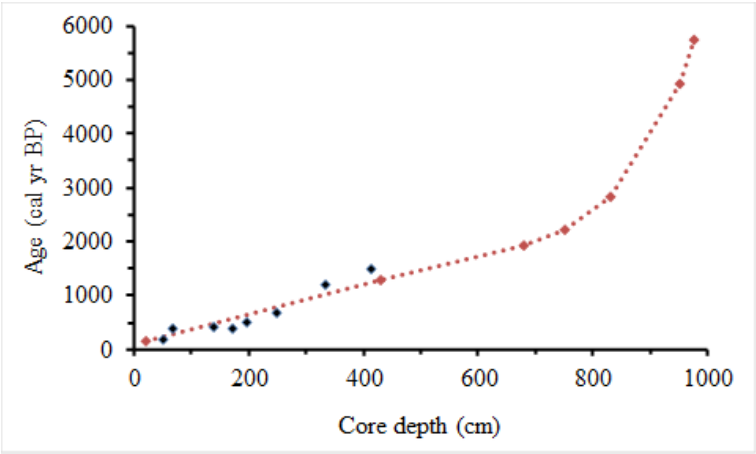

Fig. 3. Age model of Core 64PE332-30-2 based on AMS ^{14}C data (Table 1). Blue diamonds represent the ^{14}C data points of GeoB 8903.

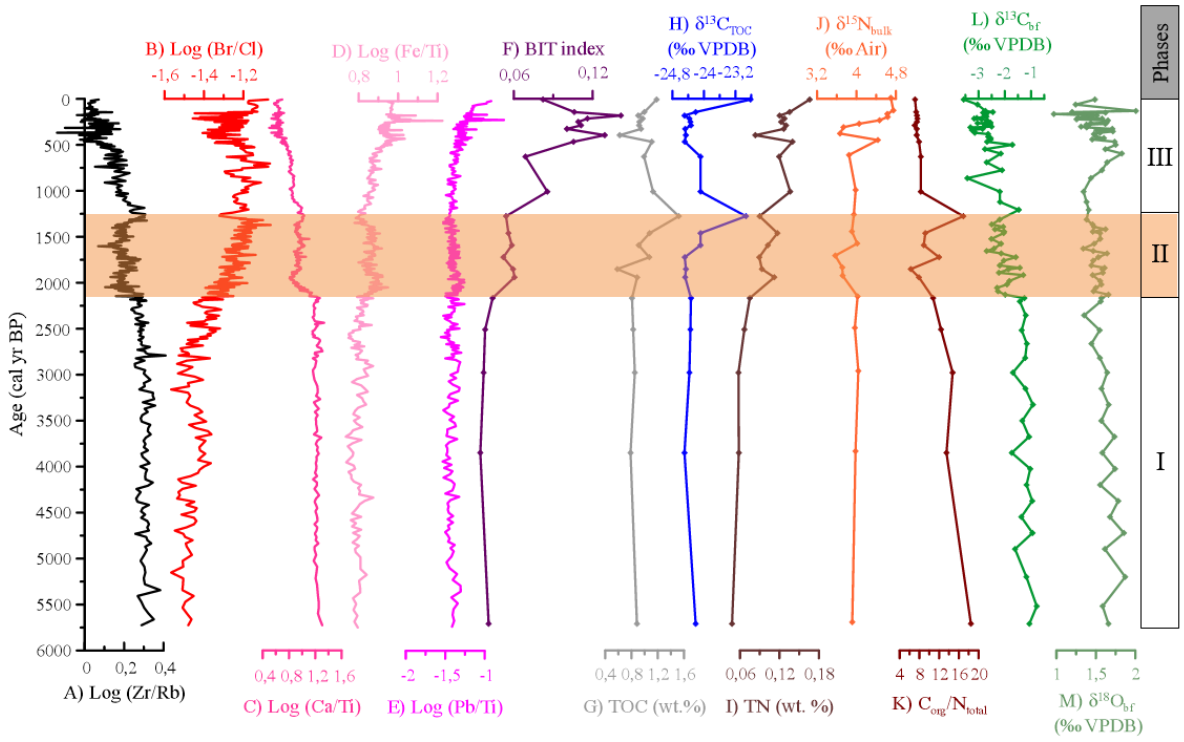

Fig. 4. Distribution of environmental parameters for the last 5750 years. XRF data: A) Zr/Rb, B) Br/Cl, C) Ca/Ti, D) Fe/Ti and E) Pb/Ti. Organic measures: F) TN, G) TOC, H) C/N ratio, I) $\delta^{15}N_{bulk}$, J) $\delta^{13}C_{TOC}$, and K) BIT index. Carbonate isotopes L) $\delta^{13}C_{bf}$ and M) $\delta^{18}O_{bf}$ analyzed for the species *N. scaphum*. The orange square indicates the limits of the three phases.

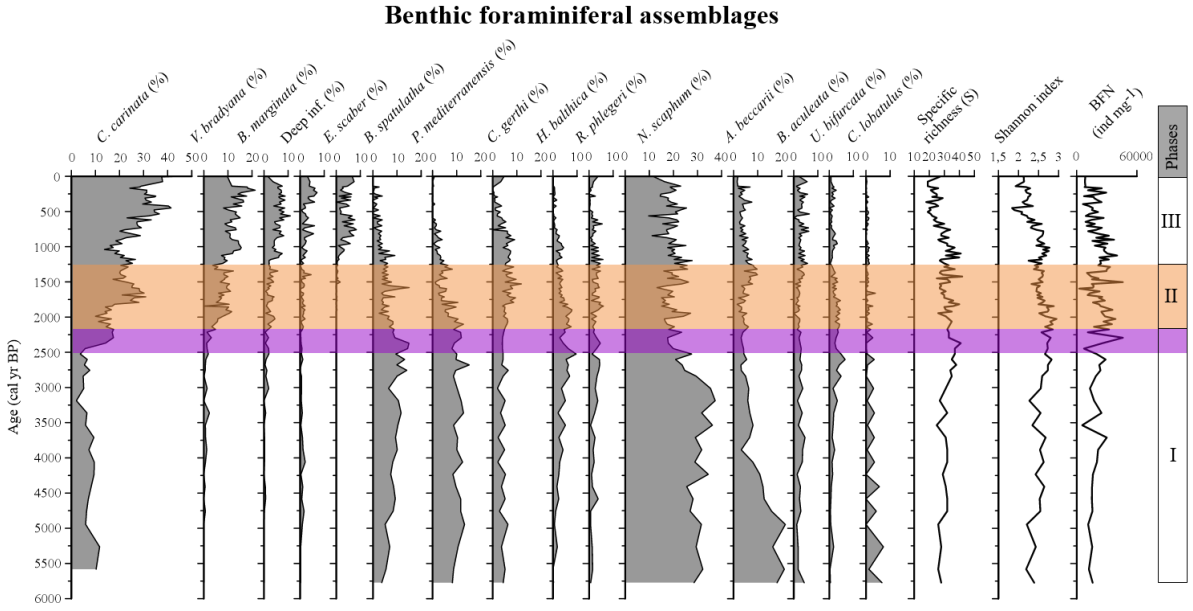

Fig. 5. Distribution of major species of benthic foraminifera (>5%) and specific richness from the 101 samples of Core 64PE332-30-2 for the last 5750 years. Deep inf. = *G. affinis* + *C. oolina*. The orange square indicates the limits of the three phases, and the purple square follows the main change of the faunal distribution.

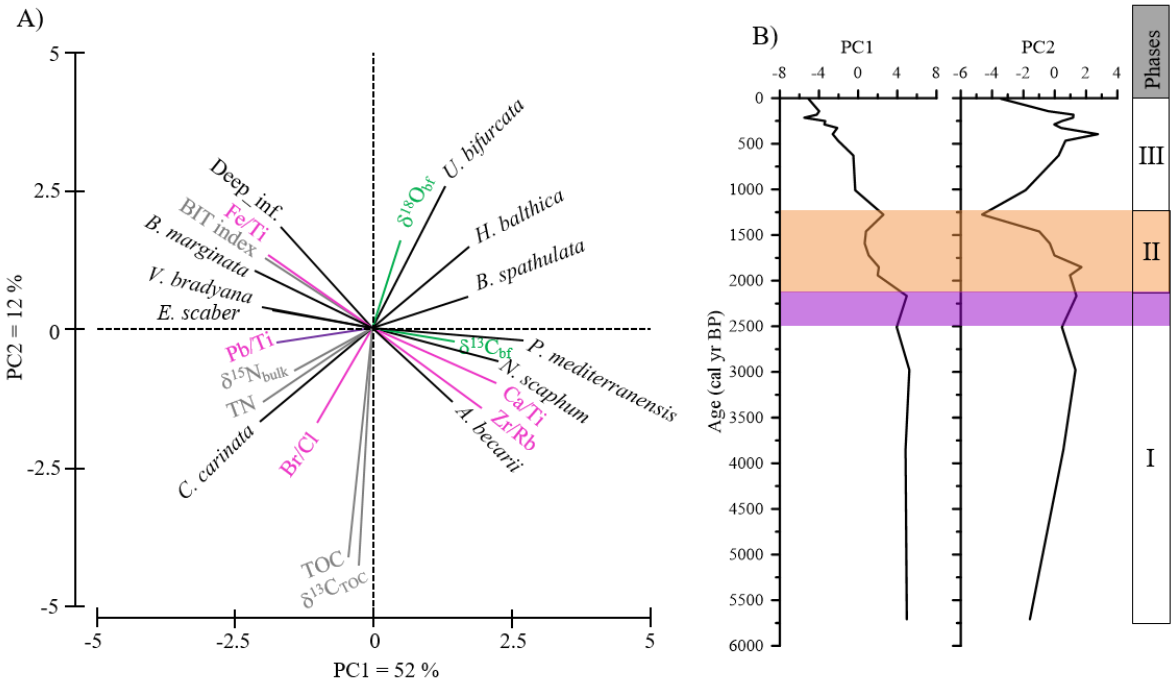

Fig. 6.A) PCA based on the major species percentages (in black), XRF data (in pink), organic compounds (in grey), and benthic foraminiferal isotopes (in green). B) Score profiles of PC1 and PC2 as a function of time. The orange square indicates the limits of the three phases, and the purple square follows the main change of the faunal distribution.

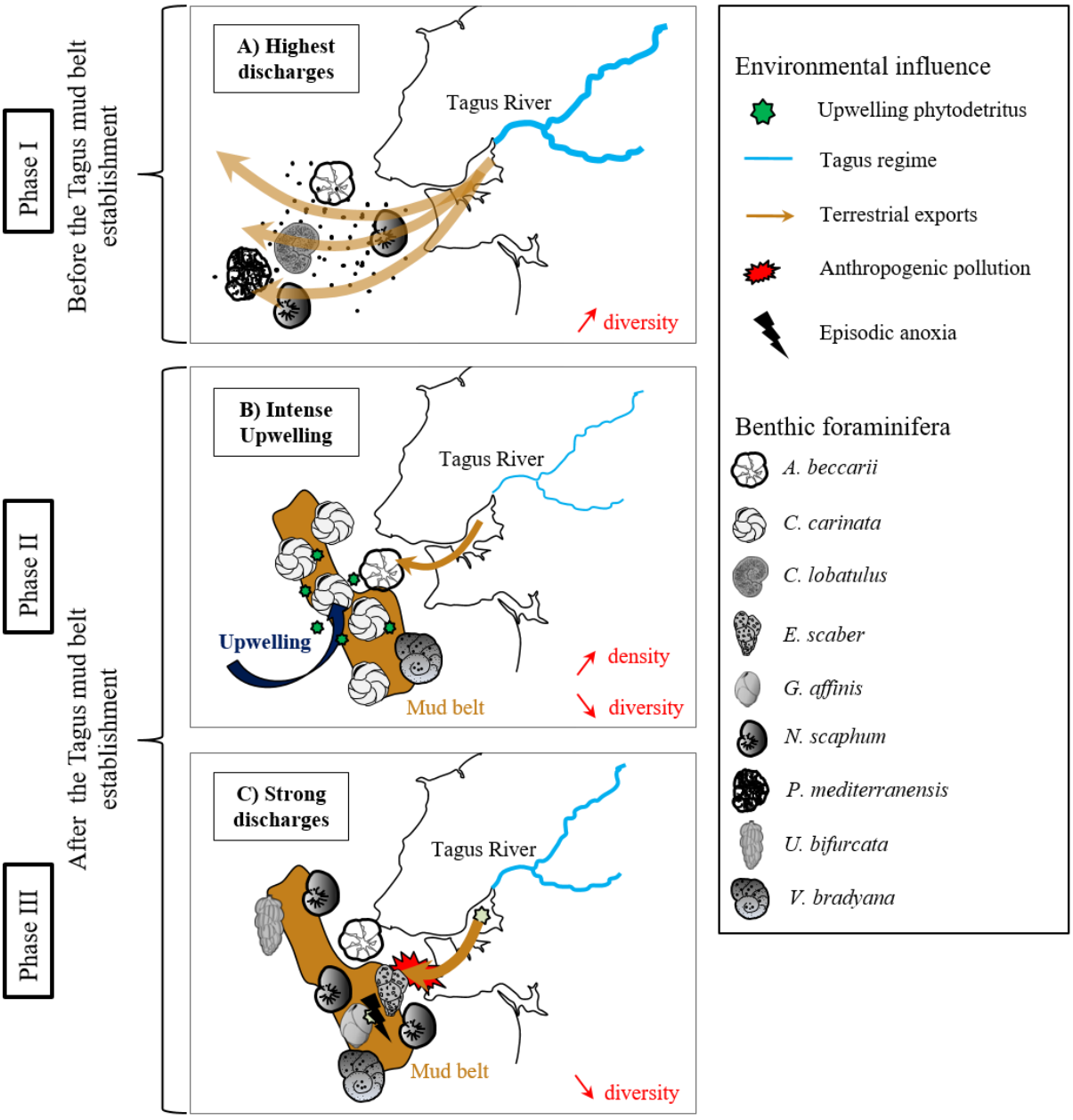

938

939 Fig. 7. Schematic representation of the three modes associated with the Tagus mud belt
940 establishment, Tagus River regime, and upwelling intensity. A) First phase, characterized by
941 very high Tagus River discharge. B) Second phase: mud belt establishment and very intense
942 upwelling activity. C) Alternating periods of strong upwelling activity and high Tagus River
943 discharge.

944

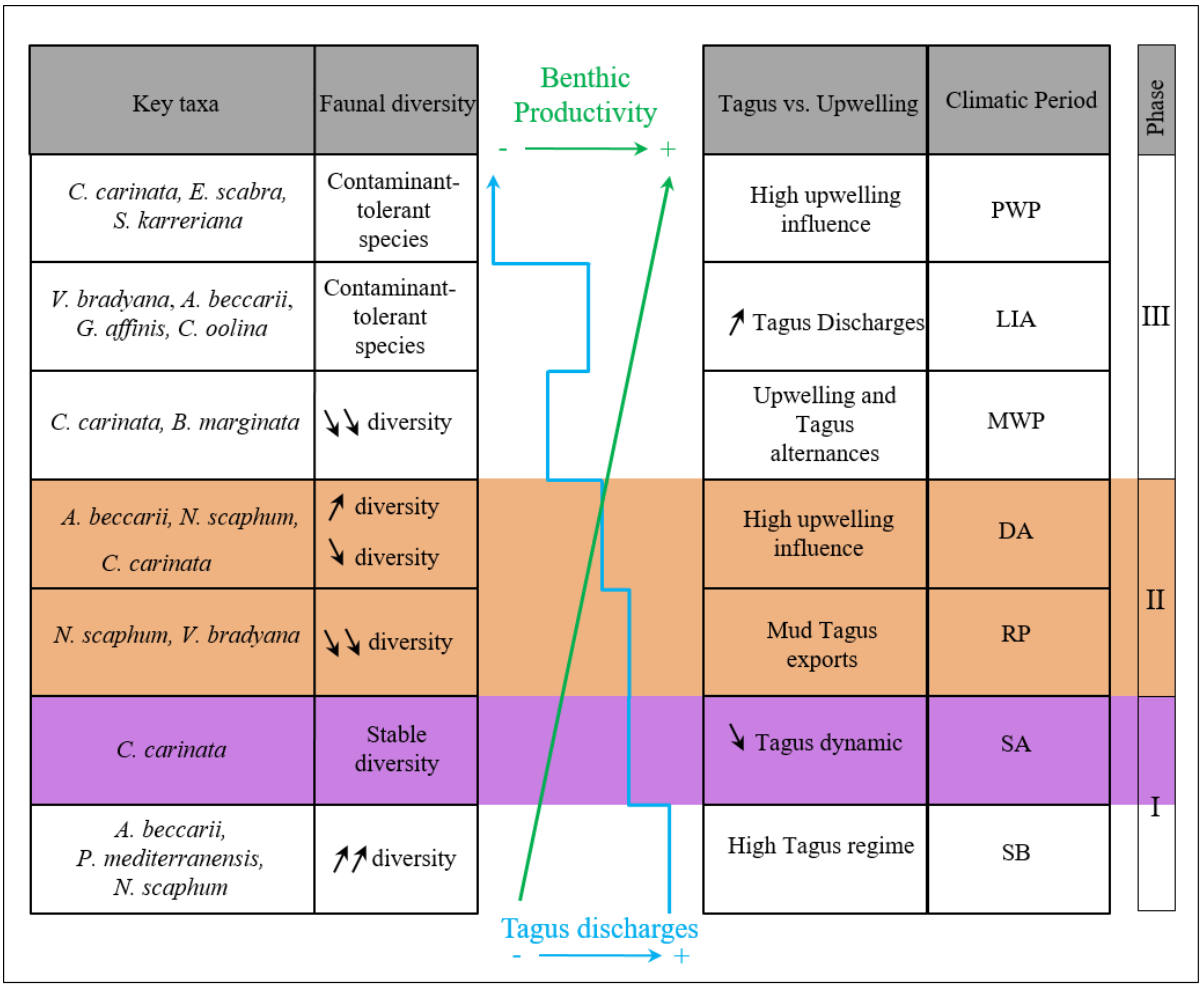

945

946 Fig. 8. Summary of the paleoenvironmental evolution of the Tagus River during the last 5750
947 years. RP = Roman Period, DA = Dark Ages, MWP = Medieval Warm Period, LIA = Little Ice
948 Age, PWP = Present Warm Period, SA = Sub-Atlantic Period, SB = Subboreal Period. The
949 orange square indicates the limits of the three phases, and the purple square follows the main
950 change of the faunal distribution.

951
952

953 Table 1. ^{14}C AMS dates of cores GeoB 8903 and 64PE332-30-2.

Sediment core	Lab no.	Core depth interval [cm]	Mean depth in core [cm]	Uncorrected AMS ^{14}C ages [cal yr BP]	Analytical error (±1σ) [yrs]	Ages (ΔR = 0 yr)(±2σ) [cal yr BP]	Ages [cal yr BP]	Analyzed material	Reference
GeoB 8903	KIA30888	52-53	51	210	35	138-223	182	Foraminifera	Alt-Epping et al. (2009)
GeoB 8903	KIA30890	65-70	69	335	55	300-501	394	Foraminifera	Alt-Epping et al. (2009)
GeoB 8903	-	139-141	140	360	25	349-456	425	Foraminifera	Alt-Epping et al. (2009)
GeoB 8903	-	171-173	172	285	30	314-408	381	Foraminifera	Alt-Epping et al. (2009)
GeoB 8903	-	198-199	198	360	45	423-498	487	Foraminifera	Alt-Epping et al. (2009)
GeoB 8903	-	248-249	248	735	30	657-726	679	Foraminifera	Alt-Epping et al. (2009)
GeoB 8903	-	333-334	333	1260	35	1121-1282	1210	Foraminifera	Alt-Epping et al. (2009)
GeoB 8903	-	413-414	413	1600	40	1390-1567	1478	Foraminifera	Alt-Epping et al. (2009)
64PE332-30-2	BETA 348791	20-22	21	500	30	41 - 235	138	Gastropod	Warden et al. (2016)
64PE332-30-2	BETA 348792	428-430	429	1730	30	1219 - 1350	1284.5	Foraminifera	Warden et al. (2016)
64PE332-30-2	BETA 348793	678-680	679	2320	30	1848 - 2033	1940.5	Gastropod	Warden et al. (2016)
64PE332-30-2	VERA-51394	750-752	751	2530	70	2122-2293	2207.5	Gastropod	This study
64PE332-30-2	VERA-51395	830-832	831	3060	70	2749-2902	2825.5	Gastropod	This study
64PE332-30-2	VERA-51396	950-952	951	4690	70	4831-5007	4919	Gastropod	This study
64PE332-30-2	BETA 317911	976-978	977	5370	30	5644 - 5850	5747	Shell fragments	Warden et al. (2016)

954 Note that ^{14}C data from GeoB 8903 were from Alt-Epping et al. (2009) and reconverted using the CALIB V0.6 with the Marine13 calibration
955 curve (Stuiver and Reimer, 1993).